Asian Journal of Basic Science & Research
Volume 5, Issue 1, Pages 41-54, January-March 2023

Zn-based Metal-Organic Frameworks (MOFs) Incorporated into Collagen-Polysaccharide-based Composite Hydrogels for Their Use in Wound Healing

Juan J. Mendoza-Villafaña[1*], Melanie G. Franco-Martínez[1], Jesús A. Claudio-Rizo[1], Denis A. Cabrera-Munguía[1], Martín Caldera-Villalobos[1], María I. León-Campos[1], Tirso E. Flores-Guía[1] & Lucía F. Cano-Salazar[1]

[1]*Facultad de Ciencias Químicas, Universidad Autónoma de Coahuila, Ing. J. Cárdenas Valdez S/N, República, 25280 Saltillo, Coahuila, México. Corresponding Author (Juan J. Mendoza-Villafaña): juan.villafana_fcq@uadec.edu.mx**

DOI: http://doi.org/10.38177/AJBSR.2023.5106

Article Received: 11 January 2023 *Article Accepted: 14 February 2023* *Article Published: 20 March 2023*

ABSTRACT

Based on the physicochemical properties of metal-organic frameworks (MOFs), and the need of having an anti-inflammatory and antibacterial effect at the same time in a material for wound healing applications, a multicomponent polymer system was synthesized. Zn-based MOFs having different amino acids acting as ligands (L-tryptophan (Trp), L-phenylalanine (Phe), and L-histidine (His)) in their coordination sphere were successfully prepared and validated by FTIR and XRD. Each MOF was incorporated into a semi-interpenetrated polymeric network (semi-IPN) based on collagen (C)-guar gum (GG)-polyurethane (PU), given composite hydrogels as end products. The physicochemical properties of these novel composite hydrogels, their *in vitro* biocompatibility, and their use as cell carriers were studied. The maximum swelling capacity was shown by CGG-Zn(Trp) while the crosslinking index was higher for CGG-Zn(Phe) and CGG-Zn(His), indicating that the chemical structure of the amino acid of the Zn-based MOF tailors these physicochemical properties. All composite hydrogels were resistant to a hydrolysis degradation process (at pH=5 and 7.4) being not entirely degraded after 14 days and having residual masses above 57%. The incorporation of Zn-based MOFs increased the biocompatibility in terms of metabolic activity and proliferation of porcine fibroblast in contact with the composite hydrogels. The low release capacity of fibroblast encapsulated inside hydrogels evaluated for 10 days indicated the non-efficient capacity of these matrixes as cell carriers, regardless of the structure of the Zn-based MOF. The strong adhesion of porcine fibroblast to the composite hydrogels is related to improving metabolic activity allowing its proliferation, making these multicomponent polymeric systems useful as efficient materials in biomedical applications such as wound dressing and tissue engineering.

Keywords: Composite hydrogels; Metal-organic frameworks (MOFs); Amino acids (AA); Zn; Polymers; Biomedicine.

1. Introduction

Multicomponent polymeric systems have gained significant academic and commercial attention, due they can provide specific characteristics that fit specific needs in the fields of biomedicine and tissue engineering. In this sense, semi-interpenetrated polymeric networks (semi-IPN) based on synthetic and natural polymers have been reported as useful multicomponent systems with applications in these fields. Specifically, in biomedical applications, these types of systems are used as implants, drug delivery systems, and regenerative medicine, among others [1–3]. Tissue repair involves in wound healing is a complex biological process that treats different stages [4,5]. Therefore, the treatments used for this purpose must fulfill the function of protecting damaged skin areas while providing an environment with a certain level of humidity, to prevent infections, eliminate exudates and favor the promotion of the healing process [6,7]. The development of new materials used as wound dressings, which meet the above issues has led to innovative research including the use and/or combination of different natural and/or synthetic polymers for this purpose [8].

Polysaccharide-based hydrogels are suitable candidates because their three-dimensional (3D) reticulated structure allows, in addition to absorbing large amounts of water, the encapsulation of bioactive molecules and cells, favoring microenvironments for cell proliferation, taking advantage of its biodegradability and biocompatibility properties [2,6]. However, even with all these advantages, some issues related to the lack of inherent antibacterial

properties, and their weak mechanical properties have led to the study of the combination of these hydrogels with other materials; one of the emerging and novel classes of hybrid materials used with this purpose are the metal-organic frameworks (MOFs), also known as porous coordination polymers. MOFs are materials consisting of metal ions or clusters linked together by organic ligands, where typically bivalent or trivalent aromatic compounds (i.e., carboxylic acids, N-aromatics, among others) form frameworks with elements such as zinc, molybdenum, copper, iron other transition metal and alkaline earth ions [9]. The applications of MOFs include energy storage, catalysis, sensors, and many others [10]; moreover, their use in biomedicine applications has proved exceptionally yielding recently [11–13]. MOF features itself or in combination with hydrogels have shown great potential as materials to accelerate the wound healing process [14,15].

2. Objectives of the Study

Considering the above, herein, novel semi-IPNs based on collagen-guar gum-polyurethane hydrogels combined with Zn-based metal-organic frameworks have been prepared. The aim of this work also involves the use of different types of amino acids (AA) as ligands (L-tryptophan (Trp), L-phenylalanine (Phe), and L-histidine (His)) during the preparation of MOFs, and therefore, the study of the physicochemical properties, and the biological activity of the composite hydrogels according to the chemical structure of the amino acid that makes up the Zinc (II) MOFs.

3. Literature Review

Composites hydrogels containing MOFs, such as MgMOF74, CaMOF74, and Zn(Atz)(Py) have been reported by our research group [16], showing high biocompatibility in terms of metabolic activity and cell proliferation (higher than 100%) for porcine fibroblasts and human monocytes, they were also fully biodegradable after 15 days and showed antibacterial activity against E. coli microorganism, a pathogen present in chronic wounds. In addition, composite hydrogels combined with MOFs revealed favorable cell signaling stimulating the secretion of important cytokines involved in wound healing (TGF-b and MCP-1). Of the three studied systems, the one that included zinc showed the best results. Zinc ion (Zn^{2+}, Zn (II)) is well known as an antibacterial agent, with good activity against bacteria, fungi, and virus [17, 18]. Also, Zn (II) is part of the trace elements required for the human body, being biocompatible and easily metabolized [19, 20]. Furthermore, it has been reported that Zn ion can participate in the anti-inflammatory process by restoring the superoxide dismutase activity, as well as inducing angiogenesis and regulating the expression of some extracellular proteins [21, 22]. These characteristics make zinc ion an ideal candidate to be used in the preparation of MOFs based on bioactive amino acids (AA) that will be used in the formulation of composite hydrogels for potential biomedical applications. In addition, the use of AA, the known monomeric units that conform proteins, acting as ligands in the building of MOFs, is highly useful for wound healing purposes due mainly to their high bioactivity and control of the different events involved in tissue healing [23–28].

4. Materials and Methods

4.1. Materials

Collagen (C) type I was obtained from porcine dermis (a1=230 000 g mol-1, a2=110, 000 g mol-1) through an enzymatic procedure [29]. Guar Gum (GG) was obtained by extracting from Cyamopsis tetragonoloba (220 000 g

mol^{-1}). Glycerol ethoxylate (1000 g mol^{-1}), Hexamethylene diisocyanate (HDI), 3-(4,5-Dimethyl-2-thiazolyl)-2,5-diphenyl-2H-tetrazolium bromide (MTT), Zinc nitrate hexahydrate [Zn(NO3)2.6H2O], 1,3,5-benzene tricarboxylic acid (BTC), L-tryptophan (Trp), L-phenylalanine (Phe) and L-histidine(His) were purchased from Merck/Aldrich and used as received. Phosphate buffer solution (PBS), Hydrochloric acid (37%), 2,2-dihydroxy-1,3 indanedione (ninhydrin) and 2-propanol were supplied from Merck/Aldrich, too. Dulbecco's Modified Eagle Medium (DMEM) and the LIVE/DEAD™ viability/cytotoxicity kit, were purchased from Thermo Fischer Scientific.

4.2. Methods

4.2.1. Synthesis of PU crosslinker

The preparation procedure for the collagen crosslinker based on polyurethane is reported elsewhere [30, 31]. Typically, the Glycerol ethoxylate (GET) was reacted at 100°C with hexamethylene diisocyanate (HDI) in a molar ratio (3:1) for 2 h. Then, sodium bisulfite aqueous solution (40 wt.%) was used to block the -NCO end groups remanent in the formed prepolymer, this process was carried during 2 h at 40°C with a constant stirring speed of 500 rpm.

4.2.2. Synthesis of Zn-based MOF (Zn-BTC-AA)

The Zn-based MOFs were prepared in a one-pot procedure by a hydrothermal method [22]. An equimolar mixture of the three main components ([$Zn(NO_3)_2.6H_2O$]: BTC: amino acid (AA)) was used. In brief, each component was dissolved in ethanol and sonicated. Then, the three solutions were placed together in an Erlenmeyer flask and mixed under constant stirring. Next, the new homogeneous solution was transferred to a Teflon-lined autoclave, and the reaction was carried out at 120°C for 12 h. Lastly, the final product was recovered by filtration, washed several times with water, and dried in an oven at 60°C. The formed Zn-based MOFs were obtained as a white solid in all cases, regardless of the type of amino acid used as ligand (Trp, Phe, or His), where each product was labeled as Zn(Trp), Zn(Phe) and Zn(His), respectively.

4.2.3. Preparation of composite hydrogels (CGG-Zn (AA))

In a general way, hydrogels were prepared as follows: 1 mL of collagen solution (6 mg mL^{-1}) was mixed with 30 µL of PU crosslinker in a 24-well culture plate at 4 °C. Then, 150 µL of GG solution (0.25 wt.% in H_2O) were added to each well containing the collagen/PU mix, and the pH of the mix was adjusted by adding 200 µL of PBS-10X. All components of the reaction were mixed vigorously for 15 minutes before incubating at 37 °C for 12 h to obtain a hydrogel with a semi-IPN structure. To obtain the different composite hydrogels, the former steps procedure was followed, however, 1 mL from a mix of Collagen/Zn (AA) (8 mL/10 mg) was used instead of pure collagen solution. The composite hydrogels were named based on the type of Zn-based MOFs used. Therefore, a set of four products (CGG, CGG-Zn(Trp), CGG-Zn(Phe), and CGG-Zn(His)) were obtained, characterized, and compared.

4.3. Physicochemical characterization and evaluation of composite hydrogels

FTIR analysis was performed on a Perkin-Elemer Frontier spectrophotometer equipped with a total attenuated reflectance accessory (ATR); 32 scans and a resolution of 4 cm^{-1} were used for the acquisitions. Analysis by

Scanning electron microscopy (SEM) was performed on a TOPCON SM-510 microscope operating at 10 kV. A ThermoScientific MultiSkan Sky spectrophotometer was used for the UV-VIS absorbance measurements. Analysis by Fluorescence microscopy was performed on a VELAB VE146YT microscope using an excitation source of λ = 441 nm.

4.3.1. Swelling capacity

Each formed composite hydrogel was weighted (by triplicated) on the initial day and the mass was registered as $\mathbf{W_1}$. Samples were let dry at room temperature, and after 24 h their mass variation was recorded, this procedure was repeated until no variation mass was observed, which was registered as $\mathbf{W_2}$. The swelling capacity was calculated by Equation 1:

$$\text{Swelling capacity } (\%) = \frac{W1-W2}{W2} * 100 \qquad (1)$$

4.3.2. Crosslinking index

1 mL of ninhydrin solution was added to each formed composite hydrogel placed in 15 mL Falcon tubes, then, 2 mL of deionized water was added to each tube, and vigorously vortex mixed before being placed in a dry bath at 90 °C for 2 h. The Falcon tubes were cooled down, and 200 µL of the supernatant of each sample (by triplication) was transferred to a 96-well culture plate and then, absorbance lectures by UV-VIS spectrophotometry at 567 nm were taken. The crosslinking index was determined by comparing the absorbances (A) of the sample (hydrogel composites) and the control sample (collagen), using Equation 2:

$$Crosslinking\ index\ (\%) = \left(1 - \frac{A_{sample}}{A_{control}}\right) * 100 \qquad (2)$$

4.3.3. Degradation profiles

Each composite hydrogel (by triplicated) initial mass was recorded ($\mathbf{W_0}$), before being immersed in falcon tubes containing 30 mL of either a PBS-1X solution (pH=7.4) or acid solution (pH=5.5). After 24 h of immersion, the samples were taken off the tubes and their mass variation were recorded ($\mathbf{W_t}$); this procedure was repeated for 14 days. The mass variation was determined by Equation 3:

$$\text{Mass variation } (\%) = \frac{W_t-W_0}{W_0} * 100 \qquad (3)$$

4.4. In vitro biological properties of hydrogel composites

4.4.1. Biocompatibility assay

The cell viability was determined by the evaluation of the metabolism of porcine dermal fibroblasts growing in contact with every hydrogel composite and by their ability to transform MTT salts in formazan [32]. 100 µL of cell suspension in DMEM culture medium (30 000 cell/mL) were added to leachates samples (100 µL) of hydrogel (CGG), composite hydrogels (CGG/Zn(AA)), and PBS-1X solution as control, each one contained in wells of a polystyrene culture plate (by triplicated). Two plate sets were prepared, one of them incubated for 24 h and the other one for 48 h, both at 37°C under sterile conditions. Once the incubation time, 10 µL of the MTT solution (1 wt.% in PBS-1X) were added to each well before incubating for another 2 h. Next, to dissolve the formed formazan

crystals, 2-propanol was used, and then, 200 µL aliquots from each sample were transferred to another 96-well culture plate, and finally, absorbance lectures were measured at 567 nm by UV-VIS spectrophotometry. Collect data (As_{ample} and $A_{control}$) were used to calculate the cell viability, where $A_{control}$ (100% of viability) corresponds to wells without hydrogels or composite hydrogels.

4.4.2. Fibroblasts carrier capacity

For the study of carrier capacity of porcine fibroblasts by the composite hydrogels CGG-Zn(AA), a new set of the products CGG, CGG-Zn(Trp), CGG-Zn(His) and CGG-Zn(Phe) were prepared as above, which were prepared in the presence of 200 µL of cell culture (30 000 cells/mL). Later, samples with and without (control) porcine fibroblasts were immersed in 30 mL of PBS-1X solution (pH=7.4) contained in 50 mL Falcon tubes and were incubated at 37°C. After 24 h of immersion under these conditions, 200 µL of each sample (by triplicate) were extracted, transferred to a 96-well culture plate, and analyzed at 558 nm by spectrophotometry. Absorbance measurements were made every 24 h for 10 days, replacing each time the extracted volumes, using PBS-1X solution to preserve the same volume for the whole incubation period. The cell turbidity measured at 558 nm is related to the cell population released at the time under study.

4.4.3. Fibroblasts proliferation

The cell proliferation assay of porcine fibroblasts on the composite hydrogels system (Collagen/ Guar Gum/Zn-based MOFs) was carried out using the LIVE/DEAD™ viability/cytotoxicity kit. 1 mL of cell suspension in DMEM culture medium was added to leachate samples (1 mL) of hydrogel (CGG), composite hydrogels (CGG/Zn(AA)), and PBS-1X solution as a control. Samples were vigorous vortex before incubating them for 48 h at 37°C, later, they were separated from the supernatant by a centrifugation process. After, 300 µL of fluorescent kit were added to samples before incubating for another 3 h at 37 °C. Finally, stained cells were transferred carefully on coverslips and were observed under a fluorescence microscope to record the green live cells and the red dead cells.

5. Results

Zn-based metal-organic frameworks used later to obtain the composite hydrogels were formed through the coordination of zinc ion, 1,3,5-benzene tricarboxylic acid (BTC), and the corresponding amino acid (AA) in the coordination sphere of zincate ions in a one-pot procedure following a hydrothermal methodology as previously described. After 12 h of reaction, white solids were recovered in each synthesized product, which were characterized by FTIR and XRD. Figure 1a shows the FTIR spectra for Zn(Trp), Zn(Phe), and Zn(His) MOFs. The FTIR spectrum of Zn(Trp), shows two absorption bands at 3510 and 3350 cm^{-1} related to the stretching vibrations of N-H bonds, a split band at around 1710-1700 cm^{-1} is attributed to the C=O carbonyl groups originated by the tryptophan and the BTC as well, the stretching bands between 1600-1400 cm^{-1} correspond to the C=C bond from the aromatic rings, while the absorption bands at 1242 cm^{-1} and 1350 cm^{-1} are attributed to C-O and C-N bonds, respectively, the former corresponding to the carboxylic acid moiety and the latter to the primary amine present in the AA. Considering that Zn (II) can retain efficiently the ligands in the coordination sphere, the observed absorptions at 750 and 970 cm^{-1} are associated with the vibration of the Zn-O coordination bond and are evidence of

the success obtention of the Zn-based metal-organic frameworks. Similar behavior was observed for the Zn(Phe) and Zn (His), where in both cases, these two absorption bands corresponding to the Zn-O coordination bond were present. Moreover, the typical broad absorption band expected for the O-H bond between 3300-2800 cm^{-1} was observed as a weaker absorption as a result of the combination between Zn^{2+} and the corresponding carboxylate groups from BTC and the AA, an effect that was more evident in the Zn(Phe) MOF, which do not contain nitrogenous atom in its aromatic ring. On the other hand, the XRD results for each synthesized MOF are presented in Figure 1b. In all cases, the presence of intense and sharp diffraction peaks indicated crystalline structures, as expected for these systems [22, 33]. Typically, when the pattern diffraction is lost, broad halos are present, which suggest the formation of large amorphous regions, not present here. Greater hierarchical arrangement is observed in the His-based MOF, since more diffraction peaks are observed in its diffractogram, which indicates that this AA generates structures with greater packing and molecular ordering than the other two AA. Structures with less molecular ordering are appreciated in the phenylalanine MOF, which indicates that the aromatic ring represents repulsion impediments with the zincate coordination sphere, therefore its FTIR spectrum presents greater intensity in the carbonyl bond band, indicating that these groups are coordinated to a lesser extent with the metal ion.

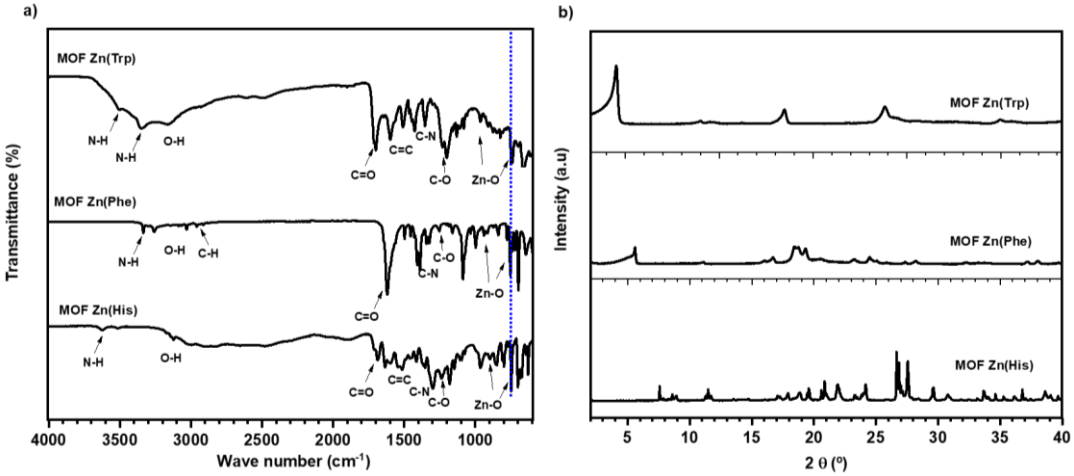

Figure 1. (a) FTIR spectra and (b) XRD patterns, of MOFs

Once the MOFs were successfully achieved, they were incorporated into the hydrogel system composed of collagen (C)-polyurethane (PU) and guar gum (GG), a semi-IPN system obtained as previously described and reported elsewhere [34]. Where C-PU is covalently bonded by urea groups while GG and MOFs will be physically associated with the matrix through hydrogen bonds and electrostatic interactions [16]. The new composite hydrogels are expected to improve their physicochemical properties, otherwise, the effectiveness of their use in wound healing applications, are depending on their biocompatibility properties, which are presented below.

In Figure 2, the maximum swelling capacity of the composite hydrogels is presented and compared with the CGG hydrogel matrix. The swelling degree showed by the CGG sample is as higher as 3783 ± 483 %, a behavior superior to observed in similar systems [34]. This superabsorbent behavior is overcome by the swell capacity shown by the composite hydrogel containing the Zn(Trp) MOF, reaching up to 4754 ± 411 %, which is probably due to the incorporation of N-H groups present in the Trp and by some free -COOH groups from the BTC ligand and AA as well, the entrapment of the Trp in this semi-IPN matrix provides more free N-H that can form hydrogen bonds with

water molecules, improving swelling. In contrast, the composite hydrogels having Zn(Phe) and Zn(His) in their formulation, showed slightly lower values than those observed by the CGG matrix, nevertheless, statistically significant differences were not observed. This behavior could be related to the hydrophobic character of the benzene rings of the phenylalanine and by the lack of protonated acid species in the carboxylated group presented in the His amino acid, for each specific MOF used. Indicating that during the polymeric semi-interpenetration process of these MOFs their polar groups are trapped in the semi-IPN matrix, decreasing the hydrophilic nature of the polymeric matrix alone.

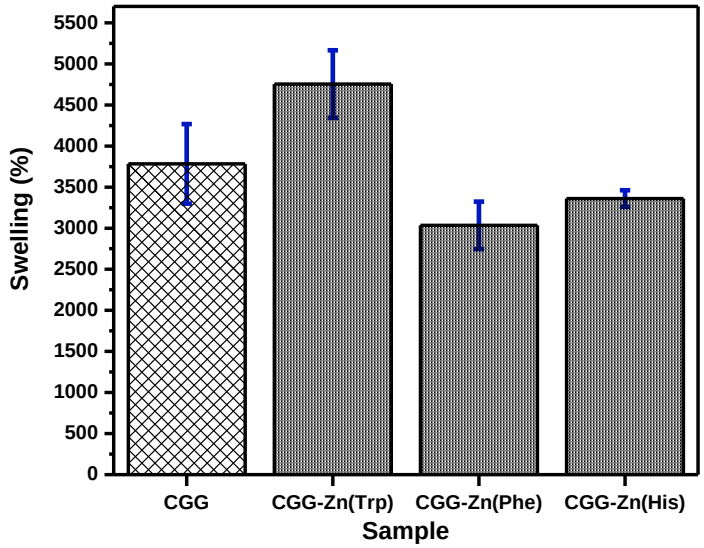

Figure 2. Maximum swelling capacity (%) of the composite hydrogels

The crosslinking index was determined for each composite hydrogel and compared against the CGG matrix (Figure 3). During the ninhydrin test, the free amino groups react with ninhydrin, which let to determine the crosslinking index indirectly. Those systems where the amino groups condense with isocyanate groups from PU, form urea links given a crosslinking structure, through covalent bonds, however, electrostatic interactions such as Van der Waals are also contributing.

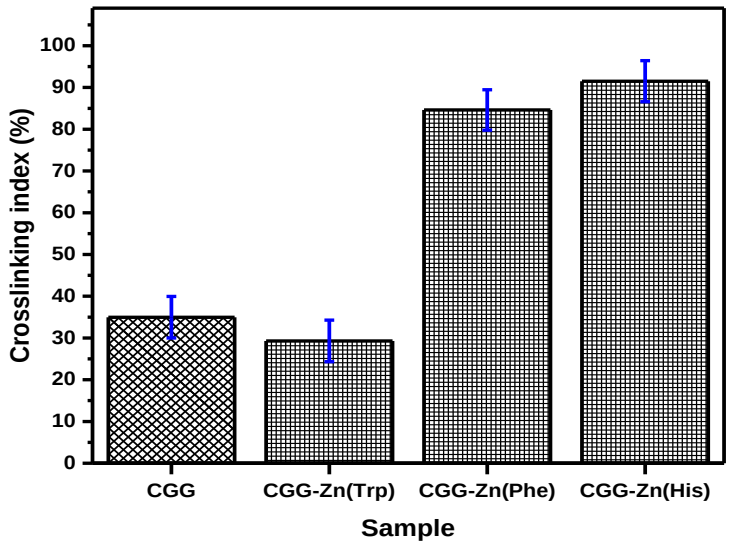

Figure 3. Crosslinking index (%) of the composite hydrogels

The crosslinking index for the composite hydrogel CGG-Zn(Trp) was 29.3 ± 5%, which is near to the CGG hydrogel (34.9 ± 5%), while the composite hydrogels CGG-Zn(Phe) and CGG-Zn(His) point out the formation of composites with higher crosslinking, having values of 84.6 ± 4.9% and 91.5 ± 4.9%, this increases up observed could be attributed to the strong interaction of the different functional groups (hydroxyl and carboxylate) of the AA with collagen amino groups mainly, which is in agreement with the slight decrease of their swelling capacity. Demonstrating that the chemical structure of the amino acid determines the crosslinking of the composite matrix. Specifically for Phe and His, the fact that they remain embedded with greater interaction during the process of polymeric semi-interpenetration favors crosslinking interactions, while in the case of Trp there are steric repulsions that do not favor this physicochemical property.

On the other hand, the degradation behavior of CGG hydrogel and CGG-Zn(AA) composite hydrogels in hydrolytic mediums (pH=5.5 and pH=7.4) is shown in Figure 4. The analysis of the curves at pH=5.5 indicated a similar degradation pattern, where mass variation (%) remains relatively stable during the first 24 hours, then, a constant degradation takes place until day 12, after that a final drop behavior was observed, having a residual mass of 66.3 %, 76.7 %, 64.1 % and 57.7 % for CGG, CGG-Zn(Trp), CGG-Zn(Phe) and CGG-Zn(His), respectively. These values indicate a slower degradation for the composite hydrogels with the MOFs Zn(Trp) and Zn(Phe), which could be related to the isoelectric point (pI_{Trp}=5.8 and pI_{Phe}=5.7) of each AA, which is near to the pH of the aqueous media. In contrast with these results, in the case of the physiological pH, the incorporation of the MOF Zn(His), which has not only a higher isoelectric point (pI=7.6), has an electrically charged side chain, as well, giving to the composite hydrogel a better stability in this hydrolytic media (pH=7.4). Both pH values were chosen due they are required for the potential use of these materials in wound healing applications, where the degradation results indicated their ability for long-term applications. The high hydrophilicity that the Zn(His)-based matrix presents is associated with greater hydrolytic degradation, while those more hydrophobic MOFs tend to decrease the rate of degradation of the composite hydrogel.

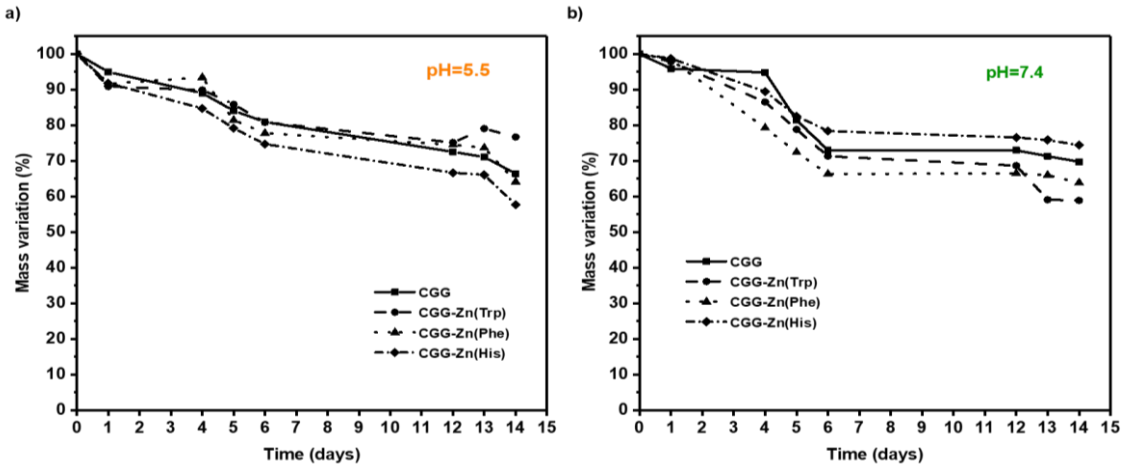

Figure 4. Degradation profiles in hydrolytic media (pH=5.5 and pH=7.4) of the composite hydrogels

The morphology of composite hydrogels was analyzed by scanning electron microscopy as shown in Figure 5. SEM micrograph of CGG hydrogel shows an amorphous fibrillar surface with the presence of some flat regions (related to GG) embedded in the collagen matrix, this is in agreement with the expected morphology for this type of

semi-IPN systems [16, 35]. In comparison, the SEM micrographs of the composite hydrogels (CGG-Zn(AA)) reveals that the presence of Zn-based MOFs modifies the fibrillary nature of the matrix, generating the presence of granulated aggregates on the surface of each composite, characterized by a larger interconnected porosity. This new morphology generated by the incorporation of MOFs is desired to guarantee adherence and growth of the cell, which is required in wound healing applications. Each type of MOF according to the chemical structure of the AA is associated with the polymeric chains generating regions with characteristic accommodation, related to crystalline surfaces (which was confirmed by DRX), larger pore size is appreciated for the hydrogel based on Zn(Phe) again indicating that the aromatic ring in this MOF promotes polymeric repulsion interactions that tend to generate structures with irregular porosity of a hydrophobic nature. Surfaces with greater homogeneity are appreciated for Zn(Trp) and Zn(His) which is attributed to the heterocyclic nitrogens that improve the microemulsion process of these MOFs in the biopolymer polymer matrix.

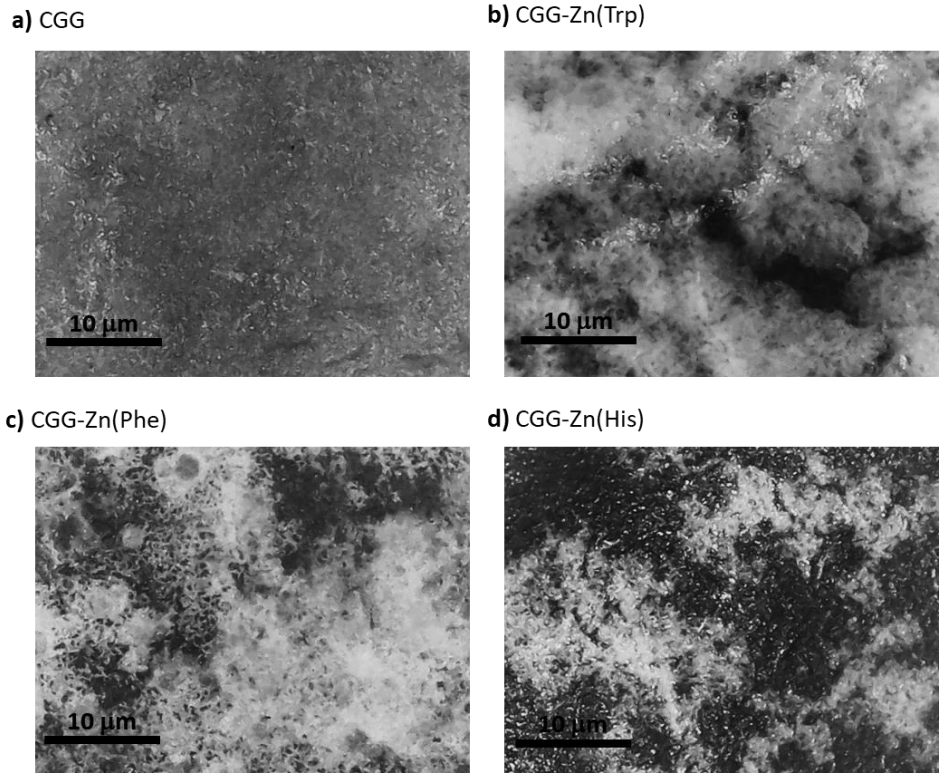

Figure 5. SEM micrographs of CGG hydrogel and CGG-Zn(AA) composite hydrogels

As mentioned above, the biocompatibility properties of CGG hydrogel and CGG-Zn(AA) composite hydrogels were evaluated through cell viability measurements using porcine dermal fibroblasts. Cell viability (%) obtained by MTT assay is shown in Figure 6a, where can be appreciated that those samples incubated during 24 h showed values higher than the control (100%), having values of 114 ± 7 %, 192 ± 14 %, 137 ± 12 % and 135 ± 14 % for CGG, CGG-Zn(Trp), CGG(Phe) and CGG(His), respectively. It can be noted that composite hydrogels do have not a cytotoxic effect over fibroblast, instead showed high biocompatibility; a similar behavior for CGG-Zn(Trp), CGG(Phe), and CGG(His) was observed, and in the case of CGG-Zn(Trp) almost twice of percent of viability compared to control was reached, indicating that the presence of this amino acid stimulates the metabolic activity of this type of cell that builds a new extracellular matrix. These results indicated that the incorporation of Zn-based

MOFs have a positive impact on fibroblast metabolism, without altering their breathing capacity when they grow in contact with the composite hydrogels, which is highly important due these cells are involved in the new tissue formation during the wound healing process [36]. In contrast, when samples were incubated for 48 h, the cell viability showed an opposite effect, which is more marked in the case of composite hydrogels having values under 50 %, pointing to a cytotoxic character, however, carrying out the proliferation test allows us to see this fact; the cells are rapidly stimulated by the composition of the biomatrix but after 48 h their metabolism decreases indicating adaptability. Literature reports consider values over 60% of cell viability as a crucial limit to be considered as non-cytotoxic materials, where cell functions as metabolism, growth, and proliferation proceed adequately [37]. This cytotoxic effect with the presence of Zn-based MOFs in the formulation of the composite hydrogels is similar regardless of the amino acid involves in, which suggests that the lack of cell viability could be related to the presence of Zinc itself. Some reports indicated that a high concentration of Zn^{2+} could inhibit the viability of fibroblasts causing serious damage to healthy cells [22, 38]. Therefore, is probably that lower MOFs concentration would be required to assure a slow release of Zn (II), avoiding them becoming harmful to healthy tissues and affecting the wound healing process.

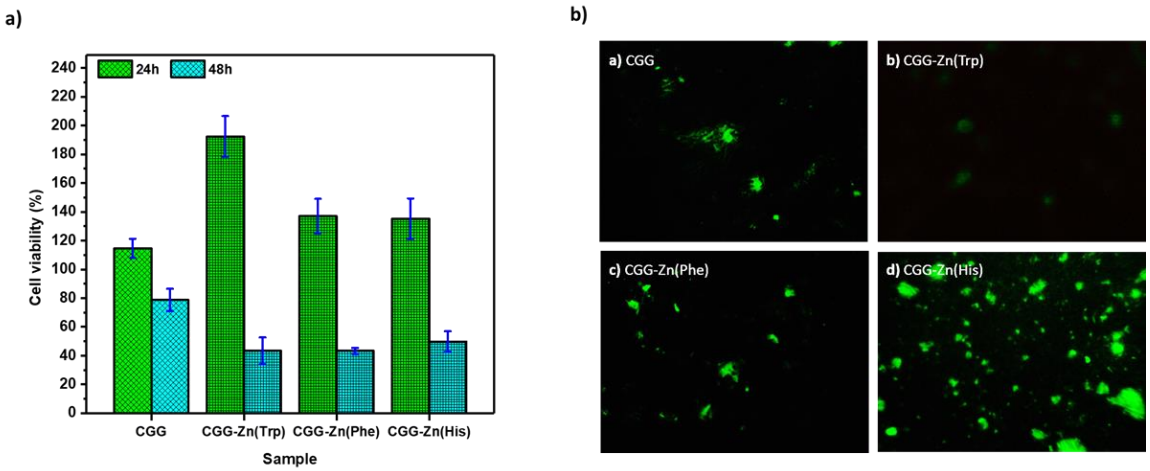

Figure 6. (a) Cell viability and (b) cell proliferation, of porcine dermal fibroblasts in contact with CGG hydrogel and CGG-Zn(AA) composite hydrogels

On the other hand, the Figure 6b shows the cell proliferation of porcine dermal fibroblasts in contact with CGG hydrogel and CGG-Zn(AA) composite hydrogels, which was carried out using the LIVE/DEAD™ kit and observed under a fluorescence microscope to record the green live cells, which grew during the first 24 h, exercising their fundamental functions as previously mentioned. Even when a cytotoxic phenomenon could occur after 48 hours of incubating, fluorescence micrographs revels cell population in all cases, being favored when Zn(His) is formulated in the composite hydrogel. These results seem not to show consistency with the viability results where cytotoxic effects that limit the breathing capacity of fibroblasts were observed, however, these contradictory results could be explained by the adaptation capacity of cells in contact with the composite hydrogels, allowing their proliferation. These proliferation results indicate that there are no effects related to cell death, since the chemical composition of the compound hydrogels under study rapidly stimulates the metabolic activity of fibroblasts, and these adapt to their composition at times longer than 24 h, allowing them to perform their

fundamental functions such as proliferation. The presence of His allows the formation of dense cell colonies proliferating on the hydrogels; indicating that the chemical structure of the MOF does have an important effect on cell growth and development. This proliferation result with Zn(His) is important, due to His amino acid is part of several proteins important in cell metabolism and duplication.

The cell carrying capacity of composite hydrogels CGG-Zn(AA) was evaluated, involving the study of controlled release of fibroblast during a period of 10 days, as shown in Figure 7. The observed release profiles indicated the absence of a significant increase in the optical density of the medium, which reveals the lack of capacity of composite hydrogels as a cell carrier. These results let to infer that under these conditions (pH=7.4), fibroblasts remain strongly attached to the CGG matrix, limiting they are released, which could be associated with their porous morphology where they can adhere, stretch and migrate, once again indicating that the surface of these new biomaterials allows the proliferation of these cells, but not their release, avoiding their use as releasers to a specific final fate. The presence of Zn-based MOFs does not make any significant difference in the release properties of the composites, despite this, these type of materials are suitable to be evaluated as efficient contaminant removers, as reported elsewhere [35].

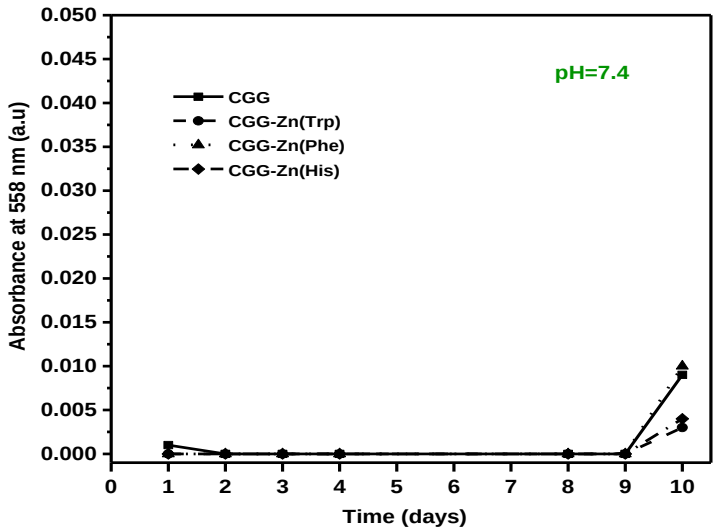

Figure 7. Porcine fibroblasts release profiles in contact with CGG hydrogel and CGG-Zn(AA) composite hydrogels

6. Conclusion

Novel multicomponent composite materials composed of Zn-based MOFs incorporated into collagen-polysaccharide-based hydrogels were successfully achieved. The obtention of different MOFs such as Zn(Trp), Zn(Phe), and Zn(His) was demonstrated by FTIR spectroscopy, highlighting the absorption at 750 and 970 cm^{-1} associated with Zn-O coordination bond, and by XRD was possible to demonstrate the presence of crystalline structures. The new composite hydrogels composed by CGG-Zn(AA) presented a porous morphology and showed a superabsorbent behavior, reaching up to 4754 ± 411 % of their swelling capacity, when Zn(Trp) was used in the formulation, while the crosslinking index was higher for CGG-Zn(Phe) and CGG-Zn(His). In addition, their degradation results at a pH=5.5 and 7.4 indicated their use for long-term applications. The cell viability (%)

obtained by the MTT assay revealed that the incorporation of Zn-based MOFs increased the biocompatibility of porcine fibroblast in contact with the composite hydrogels and allowed their proliferation as fluorescence micrographs indicated. Although the CGG-Zn(AA) composite hydrogels did not show capacity as cell carriers, their biocompatibility properties, the strong adhesion, and adaptation capacity of cells to them, indicated they could be useful as efficient materials in biomedical applications such as wound dressing and tissue engineering.

Declarations

Source of Funding

Consejo Nacional de Ciencia y Tecnología (CONACyT) supported this study with the grant FORDECYT-PRONACES/6660/2020.

Competing Interests Statement

The authors declare no competing financial, professional, or personal interests.

Consent for publication

The authors declare that they consented to the publication of this research work.

Authors' Contributions

All authors equally contributed to research and paper drafting.

Acknowledgement

The authors would like to acknowledge Consejo Nacional de Ciencia y Tecnología (CONACyT) for the grant FORDECYT-PRONACES/6660/2020.

References

[1] Thomas S, Grande D, Cvelbar U, et al. (2016). Micro- and Nano-structured Interpenetrating Polymer Networks. Thomas.

[2] Pietro Matricardi, Franco Alhaique TC. (2016). Polysaccharide Hydrogels. 1st Ed., Jenny Stanford Publishing.

[3] Crosby CO, Stern B, Kalkunte N, et al. (2022). Interpenetrating polymer network hydrogels as bioactive scaffolds for tissue engineering. Rev. Chem. Eng., 38: 347–361.

[4] García Esteo FJ, García Castellano JM, Pérez-Caballer AJ. (2005). Fundamentos de los procesos de reparación tisular: factores de crecimiento. Rev Ortop y Traumatol, 49: 5–16.

[5] Cristina De Oliveira Gonzalez A, Fortuna Costa T, De Z, et al. (2016). Wound healing - A literature review. An Bras Dermatol., 91: 614–620.

[6] Cui R, Zhang L, Ou R, et al. (2022). Polysaccharide-Based Hydrogels for Wound Dressing: Design Considerations and Clinical Applications. Front Bioeng Biotechnol., 10: 261.

[7] Torkaman S, Rahmani H, Ashori A, Najafi SHM. (2021). Modification of chitosan using amino acids for wound healing purposes: A review. Carbohydr. Polym., 258: 117675.

[8] Luo T, Tan B, Zhu L, et al. (2022). A Review on the Design of Hydrogels With Different Stiffness and Their Effects on Tissue Repair. Front Bioeng Biotechnol., 10.

[9] Zhou HCJ, Kitagawa S. (2014). Metal-Organic Frameworks (MOFs). Chem Soc Rev., 43: 5415–5418.

[10] Safaei M, Foroughi MM, Ebrahimpoor N, et al. (2019). A review on metal-organic frameworks: Synthesis and applications. TrAC - Trends Anal Chem., 118: 401–425.

[11] Yang J, Yang YW. (2020). Metal–Organic Frameworks for Biomedical Applications. Small, 16: 1906846.

[12] Shyngys M, Ren J, Liang X, et al. (2021). Metal-Organic Framework (MOF)-Based Biomaterials for Tissue Engineering and Regenerative Medicine. Front Bioeng Biotechnol., 9: 96.

[13] Haider J, Shahzadi A, Akbar MU, et al. (2022). A review of synthesis, fabrication, and emerging biomedical applications of metal-organic frameworks. Biomater Adv., 140: 213049.

[14] Asadniaye Fardjahromi M, Nazari H, Ahmadi Tafti SM, et al. (2022). Metal-organic framework-based nanomaterials for bone tissue engineering and wound healing. Mater Today Chem., 23: 100670.

[15] Wang L, Xu H, Gao J, et al. (2019). Recent progress in metal-organic frameworks-based hydrogels and aerogels and their applications. Coord Chem Rev., 398: 213016.

[16] Caldera-Villalobos M, Cabrera-Munguía DA, Becerra-Rodríguez JJ, Claudio-Rizo JA. (2022). Tailoring biocompatibility of composite scaffolds of collagen/guar gum with metal–organic frameworks. RSC Adv.

[17] Pasquet J, Chevalier Y, Pelletier J, et al. (2014). The contribution of zinc ions to the antimicrobial activity of zinc oxide, Colloids Surfaces. A Physicochem Eng Asp., 457: 263–274.

[18] Gudkov S V., Burmistrov DE, Serov DA, et al. (2021). A Mini Review of Antibacterial Properties of ZnO Nanoparticles. Front Phys., 9: 49.

[19] Stefanidou M, Maravelias C, Dona A, Spiliopoulou C. (2006). Zinc: A multipurpose trace element. Arch Toxicol., 80: 1–9.

[20] Chitturi R, Baddam VR, Prasad L, et al. (2015). A review on role of essential trace elements in health and disease. J Dr NTR, Univ Heal Sci., 4: 75.

[21] Jarosz M, Olbert M, Wyszogrodzka G, et al. (2017). Antioxidant and anti-inflammatory effects of zinc, Zinc-dependent NF-κB signaling. Inflammopharmacology, 251(25): 11–24.

[22] Chen Y, Cai J, Liu D, et al. (2022). Zinc-based metal organic framework with antibacterial and anti-inflammatory properties for promoting wound healing. Regen Biomater.

[23] Barouti N, Mainetti C, Fontao L, Sorg OL. (2015). Tryptophan as a Novel Potential Pharmacological Treatment for Wound Healing via Aryl Hydrocarbon Receptor Activation. Dermatology, 230: 332–339.

[24] Jonckheere D, Steele JA, Claes B, et al. (2017). Adsorption and Separation of Aromatic Amino Acids from Aqueous Solutions Using Metal-Organic Frameworks. ACS Appl Mater Interfaces, 9: 30064–30073.

[25] Chen S, Lu J, You T, Sun D. (2021). Metal-organic frameworks for improving wound healing. Coord Chem Rev., 439: 213929.

[26] Lin Z, Li R, Liu Y, et al. (2020). Histatin1-modified thiolated chitosan hydrogels enhance wound healing by accelerating cell adhesion, migration and angiogenesis. Carbohydr Polym., 230: 115710.

[27] Torkaman S, Rahmani H, Ashori A, Najafi SHM. (2021). Modification of chitosan using amino acids for wound healing purposes: A review. Carbohydr Polym., 258: 117675.

[28] Li M, Qiu W, Wang Q, et al. (2022). Nitric oxide-releasing L-Tryptophan and L-Phenylalanine based Poly(ester urea)s electrospun composite mats as antibacterial and antibiofilm dressing for wound healing. Compos Part B, Eng., 229: 109484.

[29] Claudio-Rizo JA, Rangel-Argote M, Castellano LE, et al. (2017). Influence of residual composition on the structure and properties of extracellular matrix derived hydrogels. Mater Sci Eng C, 79: 793–801.

[30] Mendoza-Novelo B, Mata-Mata JL, Vega-González A, et al. (2014). Synthesis and characterization of protected oligourethanes as crosslinkers of collagen-based scaffolds. J Mater Chem B, 2: 2874–2882.

[31] Claudio-Rizo JA, Mendoza-Novelo B, Delgado J, et al. (2016). A new method for the preparation of biomedical hydrogels comprised of extracellular matrix and oligourethanes. Biomed Mater., 11.

[32] Lopéz-Martínez EE, Claudio-Rizo JA, Caldera-Villalobos M, et al. (2022). Hydrogels for Biomedicine Based on Semi-Interpenetrating Polymeric Networks of Collagen/Guar Gum: Applications in Biomedical Field and Biocompatibility. Macromol Res., 30: 384–390.

[33] He J, Zhang G, Xiao D, et al. (2012). Helicity controlled by the chirality of amino acid: two novel enantiopure chiral 3D architectures containing fivefold interwoven helices. Cryst Eng Comm., 14: 3609–3614.

[34] Lopéz-Martínez EE, Claudio-Rizo JA, Caldera-Villalobos M, et al. (2022). Hydrogels for Biomedicine Based on Semi-Interpenetrating Polymeric Networks of Collagen/Guar Gum: Synthesis and Physicochemical Characterization. Macromol Res., 30: 375–383.

[35] Caldera-Villalobos M, Cabrera-Munguía DA, Flores-Guía TE, et al. (2021). Removal of water pollutants using composite hydrogels comprised of collagen, guar gum, and metal-organic frameworks. J Polym Res., 28: 1–19.

[36] Komi DEA, Khomtchouk K, Santa Maria PL. (2020). A Review of the Contribution of Mast Cells in Wound Healing: Involved Molecular and Cellular Mechanisms. Clin Rev Allergy Immunol., 58: 298–312.

[37] Amaya-Chantaca NJ, Caldera-Villalobos M, Claudio-Rizo JA, et al. (2022). Semi-IPN hydrogels of collagen and gum arabic with antibacterial capacity and controlled release of drugs for potential application in wound healing. Prog Biomater., Pages 1–16.

[38] Song W, Zhang J, Guo J, et al. (2010). Role of the dissolved zinc ion and reactive oxygen species in cytotoxicity of ZnO nanoparticles. Toxicol Lett., 199: 389–397.